Molecular engineering of a cobalt-based electrocatalytic nanomaterial for H_2 evolution under fully aqueous conditions

Eugen S Andreiadis, Pierre-André Jacques, Phong D Tran, Adeline Leyris, Murielle Chavarot-Kerlidou, Bruno Jousselme, Muriel Matheron, Jacques Pécaut, Serge Palacin, Marc Fontecave, et al.

Supporting Information

Molecular Engineering of a Cobalt-based Electrocatalytic Nano-Material for H_2 Evolution under Fully Aqueous Conditions

Eugen S. Andreiadis,[a] Pierre-André Jacques,[a] Phong D. Tran,[a] Adeline Leyris,[c] Murielle Chavarot-Kerlidou,[a] Bruno Jousselme,[b] Muriel Matheron,[c] Jacques Pécaut,[d] Serge Palacin,[b] Marc Fontecave[a, e] and Vincent Artero[*a]

[a] *Laboratoire de Chimie et Biologie des Métaux (CEA / Université Grenoble 1 / CNRS), 17 rue des Martyrs, F-38054 Grenoble CEDEX 9, France*

[b] *CEA, IRAMIS, SPCSI, Chemistry of Surfaces and Interfaces group, F-91191 Gif sur Yvette CEDEX, France*

[c] *Department of Technology for Biology and Health, CEA LETI-MINATEC, 17 rue des Martyrs, F-38054 Grenoble CEDEX 9, France*

[d] *CEA, INAC, LCIB (UMR-E 3 CEA / UJF-Grenoble 1), 17 rue des Martyrs, F-38054 Grenoble CEDEX 9, France*

[e] *Collège de France, 11 place Marcelin-Berthelot, F-75231 Paris CEDEX 5, France.*

[*] To whom correspondence may be addressed:

Fax: +33 4 38 78 91 24; Tel: +33 4 38 78 91 06; E-mail: vincent.artero@cea.fr

Table of contents

Experimental

General methods and chemicals used. Solvents and starting materials were purchased from Sigma-Aldrich and used without further purification, unless otherwise stated. When necessary, solvents were distilled under argon: diethylether was distilled by refluxing over Na/benzophenone; dry acetonitrile and dichloromethane were obtained by distillation on CaH_2. The (4-aminoethyl)benzenediazonium tetrafluoroborate salt was prepared as previously described.[1] All reactions in solution were routinely performed under an inert atmosphere of argon using conventional vacuum-line and glasswork techniques. The metal complexes were however handled in air in the solid state. Commercial grade NC3100 multi-walled carbon nanotubes (MWCNT) were obtained from Nanocyl (purity >95% in carbon) and used as received. The gas diffusion layer (GDL) substrate was purchased from GORE Fuel Cell Technologies (CARBEL CL-P-02360).

General characterization methods and equipment. ^{1}H NMR spectra were recorded at 298 K in 5 mm o.d. tubes on a Bruker AC 300 spectrometer equipped with a QNP probehead operating at 300.0 MHz for ^{1}H and 75.5 MHz for ^{13}C. Chemical shifts reported in ppm are given relative to TMS and were referenced internally to the residual solvent resonance. Mass spectra were run on a Thermo Scientific LXQ mass spectrometer equipped with an electrospray source. High resolution mass spectra and elemental analyses were performed by the Service Central d'Analyses of CNRS (Vernaison, France). SEM images showing the electrode morphology were recorded with a FEG-SEM (Leo 1530) operating at 5 kV and equipped with a Princeton Gamma-Tech EDX system operating at 15 kV.

X-ray photoemission spectroscopy (XPS). The analyses were performed with a Kratos Axis Ultra DLD using a high-resolution monochromatic Al-Kα line X-ray source at 1486.6 eV. Fixed analyzer pass energy of 20 eV was used for core level scans. Survey spectra were captured at pass energy of 160 eV. The photoelectron take-off angle was always normal to the surface, which provided an integrated sampling depth of approximately 15 nm. All spectra were referenced with an external gold substrate with a binding energy of 84.0 eV for Au 4f.

X-ray crystallography. Diffraction data were collected using an Oxford Diffraction XCallibur S Kappa area detector four-circle diffractometer (Mo-Kα radiation $\lambda = 0.71073$ Å, graphite monochromator), controlled by the Oxford Diffraction CrysAlis CCD software.[2] Unique intensities with $I > 10\sigma(I)$ detected on all frames using the Oxford Diffraction RED were used to refine the

values of the cell parameters. The substantial redundancy in data allows empirical absorption corrections to be applied using multiple measurements of equivalent reflections with the Oxford Diffraction ABSPACK. The space group was determined from systematic absences, and it was confirmed by the successful resolution of the structure. The structure was solved by direct methods using the Bruker SHELXTL 6.14 package[3] and all the atoms were found by difference Fourier syntheses. All non-hydrogen atoms were anisotropically refined on *F*. Hydrogen atoms were fixed in ideal positions, except for the oxime hydrogen which was refined isotropically. X-ray suitable crystals of **2**·0.3H_2O were grown by slowly evaporating an acetonitrile/water solution. The asymmetric unit contains a molecule of **2** with the propylene moiety disordered over two positions with relative occupancies 0.834(6) / 0.166(6) and the azide moiety also disordered over two positions with relative occupancies 0.906(3) /0.094(3), as well as 0.312(6) water molecules in partial occupation. Analysis of the CIF related to **2**·0.3H_2O (CCDC 896938) with CheckCIF does not display any A alert and only one B alert. The latter indicates that the thermal coefficients of nitrogen atoms of the azide moiety are too anisotropic. This is related to the fact that the propylene bridge and the azide moiety are both disordered.

Experimental details for X-ray data collection: formula C11 H18 Cl2 Co N7 O2.31; FW = 415.15 $g \cdot mol^{-1}$; T = 150(2)K; crystal system monoclinic; space group P $2_1/n$; unit cell dimensions a = 10.06772(19) Å, b = 14.6157(3) Å, c = 11.4658(2) Å, β = 97.5274(18) deg,; V = 1672.62(5) $Å^3$; Z = 4; ρ = 1.688 $g \cdot cm^3$; μ = 1.372 mm^{-1}; θ range 3.58 to 30.51°; reflns. collected 9728; indep. reflns. 5026; parameters 273; GOF on F^2 1.015; final R indices [I>2sigma(I)] R1 = 0.0307, wR2 = 0.0744; R indices (all data) R1 = 0.0455, wR2 = 0.0771 with wR2 = $[\Sigma[w(F_0^2 - F_c^2)^2] / \Sigma w(F_0^2)^2]^{1/2}$, where $w^{-1} = [\Sigma(F_0^2) + (aP)^2 + bP]$ and $P = [\max(F_0^2, 0) + 2F_c^2]/3$.

Electrochemical measurements. Electrochemical analysis was performed using a BioLogic SP300 bi-potentiostat controlled via the EC-Lab® V9 software. For measurements in organic solvents (acetonitrile), the instrument was fitted with a high current/high voltage board (1 A/48 V). The electrochemical experiments were carried out in three-electrode electrochemical cells under nitrogen atmosphere using glassy carbon (GC) or the original modified electrodes described in the experimental part as the working electrode. A platinum-grid placed in a separate compartment connected by a glass-frit and filled with the electrolytic solution was used as auxiliary electrode. The reference electrodes were based either on the Ag/AgCl/KCl 3M couple (Ag/AgCl) for measurements in acetonitrile ($E°_{Ag/AgCl}$ = 0.210 V vs NHE), or on the Hg/Hg_2Cl_2/KCl couple (SCE)

for measurements in aqueous solutions ($E°_{SCE}$ = 0.240 V vs NHE). The potential has been calibrated after each experiment by adding either ferrocene (when using organic solvents) or potassium ferrocyanide (when using aqueous solutions) and measuring its half-wave potential. The potential of the Reversible Hydrogen Electrode (RHE) is defined as $E°_{RHE} = -0.059 \cdot pH$. Thus potentials measured versus the SCE electrode can be converted versus the RHE by using the following formula: $E_{vs\ RHE} = E_{vs\ SCE} + E°_{SCE} + 0.059 \cdot pH$. For acid catalysis measurements, additions of anilinium tetrafluoroborate aliquots were done by syringe from concentrated solutions of the acid in acetonitrile, in order to minimize dilution effects.

Determination of the rate of H_2 production

During controlled-potential coulometry and linear sweep voltammetry experiments, we analysed H_2 evolution with a Perkin-Elmer Clarus 500 gas chromatograph equipped with a porapack Q 80/100 column (6' 1/8") thermostated at 40 °C and a TCD detector thermostated at 100 °C. The GC was mounted in the so called "continuous flow" mode, where a continuous stream of carrier gas flushes the gas-tight electrochemical cell in permanence at a given rate D (5 mL.min^{-1}). This stream fills an injection loop of a given volume V (here 100µL) in the GC. The contents of the injection loop is fed at given intervals Δt (here 2 minutes) into the GC that measures the concentration of H_2 contained within the sample. Assuming that the concentration of the species in the gas phase varies slowly during the interval Δt (which can be verified *a posteriori* by looking at successive samplings), the rate at which a given gas is extracted from the electrochemical cell is simply given by:

$$v_g^e = C_g \times D$$

where C_g is the concentration of gas g measured by the GC and v_g^e is the rate at which the gas is *extracted* from the cell. As the gas extraction system is linear, this extraction rate is related to the rate at which the gas is *produced* (v_g^p) in the electrochemical cell through the system response function, $g(t)$:

$$v_g^e(t) = \int_0^t v_g^p(t - t')g(t')\,\mathrm{d}t'$$

To obtain v_g, one has to determine the response function, by injecting a determined quantity of gas in the cell at a given time and recording the response, and then use it to deconvolve the signal using FFT. In practice however, we found that the response function time scale (a few minutes) was significantly faster than the time scale of the variations of gas production, in which case one has $v_g^p \approx v_g^e$. This is why we plotted directly v_g^e (normalized by the electrode geometric surface in order to compare to the current density) on Figure 4 and S6. A control calibration was also performed via chrono-potentiometric experiments involving a platinum working electrode immersed in a 0.1M sulfuric acid solution, for which the Faradaic yield of H_2 production was considered to be unitary.

Synthesis

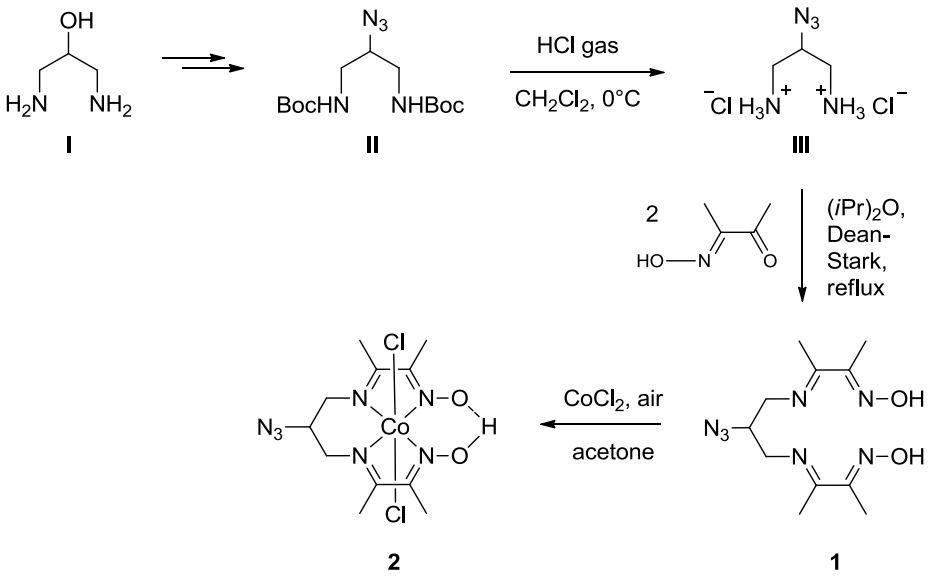

N,N'-di-*t*-boc-2-azido-1,3-diaminopropane **II** (boc = butyloxycarbonyl) was prepared in 3 steps from commercially available 2-hydroxy-1,3-diaminopropane according to a literature reference.[4]

2-azido-1,3-diaminopropane hydrochloride salt (**III**). The compound was prepared according to a modified literature procedure.[4] Dry HCl was bubbled for 2 h in a solution of **II** (2g, 6.3 mmol) in CH_2Cl_2 at 0°C. The resulting white precipitate was filtered and washed with Et_2O, dried under vacuum and used without further purification (1.13 g, 95%). ^{1}H NMR (300 MHz, D_2O): δ ppm 4.28 (ddd, J = 12.8, 9.3, 3.7 Hz, 1H, CH–N_3), 3.38 (dd, J = 13.6, 3.8 Hz, 2H, CH_2), 3.15 (dd, J = 13.6, 9.1 Hz, 2H, CH_2).

N^2,N^2'-2-azidopropanediylbis(2,3-butadione-2-imine-3-oxime) (**1**). A solution of **III** (400 mg, 2.1 mmol), 2,3-butadione-monoxime (424 mg, 4.2 mmol) and $NaHCO_3$ (360 mg, 4.2 mmol) in a biphasic mixture of water (5 ml) and $^{i}Pr_2O$ (20 mL) was refluxed overnight using a Dean-Stark apparatus. The hot reaction mixture was filtered and the precipitate washed with CH_2Cl_2. The filtrate was evaporated under reduced pressure. The resulting solid was dissolved in a minimum of AcOEt, precipitated by addition of pentane, filtered and dried under vacuum (300 mg, 51%). ^{1}H NMR (300 MHz, DMSO d^6): δ ppm 11.55 (s, 2H, N–OH); 4.03–4.00 (m, 1H, CH–N_3); 3.64–3.59 (m, 4H, CH_2); 2.03 (s, 6H, CH_3); 1.94 (s, 6H, CH_3). ^{13}C NMR (75 MHz, DMSO d^6): δ ppm 166.0, 156.8, 63.4, 53.9, 13.9, 9.4. HR-MS (ESI^+): *m/z* calcd for $C_{11}H_{20}N_7O_2$ 282.1673; found 282.1679 $[M+H]^+$.

[Co(DO)(DOH)N_3-pnCl_2] (**2**). To a solution of ligand **1** (197 mg, 0.70 mmol) in acetone (20 mL) was added a solution of $CoCl_2 \cdot 6H_2O$ (166 mg, 0.70 mmol) in acetone (10 mL). The mixture was stirred for 2 h under a continuous bubbling of air. The resulting green precipitate is filtered off, dissolved in CH_3CN, filtered and the solvent evaporated. The same operation was done with CH_2Cl_2 to finally yield a green powder (227 mg, 79% yield). ^{1}H NMR (300 MHz, acetone d^6): δ ppm 19.40 (s, 1H, OHO); 4.62–4.53 (m, 3H, CH_2, CHN_3); 3.88 (t, 13.2 Hz, 2H, CH_2); 2.77 (d, J = 1.7 Hz, 6H, CH_3); 2.55 (s, 6H, CH_3). ^{13}C NMR (75 MHz, DMSO d^6): δ ppm 176.9, 155.9, 58.6, 54.0, 18.2, 13.7. MS (ESI^-): *m/z* 407.8 $[M-H]^-$. Elemental analysis calcd. (%) for $C_{11}H_{18}Cl_2CoN_7O_2 \cdot 0.4\ C_3H_6O$: C 33.70, H 4.72, N 22.72; found: C 33.34, H 4.60, N 22.35.

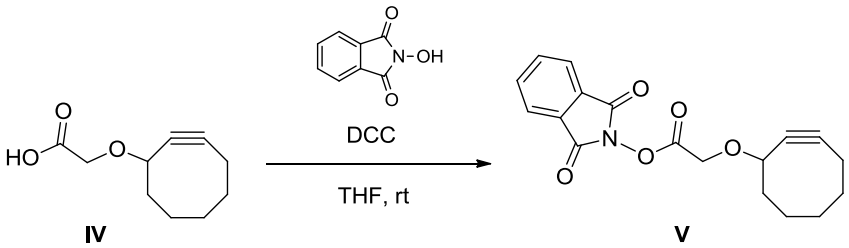

IV **V**

N-phthalimidyl-2-(cyclooct-2-yn-1-yloxy)acetate (**V**)**.** The 2-(cyclooct-2-yn-1-yloxy)acetic acid precursor **IV** was custom-synthesized by Oribase-pharma according to Bertozzi's procedure.[5] A mixture of **IV** (235 mg, 1.22 mmol), *N*-hydroxyphthalimide (206 mg, 1.22 mmol) and *N,N'*-dicyclohexylcarbodiimide (255 mg, 1.22 mmol) in distilled THF (15 mL) cooled in an ice bath was allowed to reach room temperature and stirred overnight under argon. The resulting fine white precipitate was filtered off, washed with CH_2Cl_2 and the filtrate evaporated and dried. The oily product is redissolved in a minimum of CH_2Cl_2, filtered, evaporated and dried under vacuum to give

a white product (395 mg, 99%). ^{1}H NMR (300 MHz, CD_2Cl_2): δ ppm 7.93 – 7.77 (m, 4H, Ph), 4.52 (dd, *J* = 40.1, 17.0 Hz, 2H, CH_2-O), 4.47 – 4.43 (m, 1H, CH-O), 2.35 – 1.06 (m, 10H, CH_2^{oct}). ^{13}C NMR (75 MHz, CD_2Cl_2): δ ppm 167.39, 162.15, 135.50, 129.29, 124.48, 102.91, 91.15, 74.00, 64.57, 42.67, 34.79, 30.13, 26.64, 21.12. MS (ESI^+): *m/z* 350.3 [$M+Na^+$].

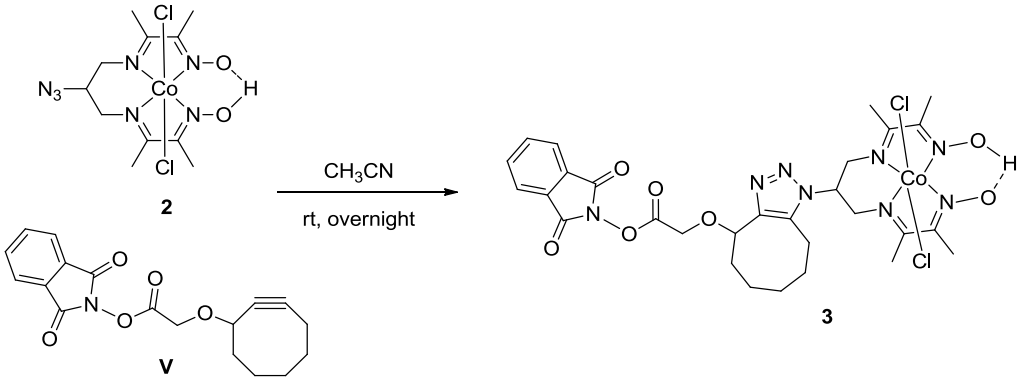

[Co(DO)(DOH)C_8-pnCl_2] (**3**)**.** A solution of **2** (200 mg, 0.48 mmol) and **V** (165 mg, 1 equiv.) in distilled CH_3CN (15 mL) was stirred at room temperature for 24 hours. After concentration under vacuum, the reaction mixture was purified on a Sephadex LH20 column (eluent: acetone / CH_2Cl_2, 1/1). The first fractions were evaporated and dried under vacuum to give a green powder (279 mg, 75 %). ^{1}H NMR (300 MHz, acetone d^6): δ ppm 19.45 (s, 1H, OH), 7.98 (s, 4H, Ph), 5.80 – 5.52 (m, 1H, CH-O), 5.06 (ddd, *J* = 12.0, 7.7, 3.5 Hz, 1H, CH-N), 4.77 (dd, *J* = 27.3, 16.8 Hz, 2H, CH_2-N), 4.66 (s, 2H, CH_2-O), 4.75 – 4.39 (m, 2H, CH_2-N), 3.06 (dtd, *J* = 21.8, 14.9, 7.0 Hz, 2H, CH_2^{oct}), 2.68 (dd, *J* = 31.3, 1.2 Hz, 6H, CH_3), 2.59 (d, *J* = 11.8 Hz, 6H, CH_3), 2.30 – 2.19 (m, 1H, CH_2^{oct}), 1.99 – 1.91 (m, 1H, CH_2^{oct}), 1.87 – 1.13 (m, 6H, CH_2^{oct}). MS (ESI^+): *m/z* 701.3 [$M-Cl^-$]. Elemental analysis calcd. (%) for $C_{29}H_{35}Cl_2CoN_8O_7 \cdot 0.5\ CH_2Cl_2$: C 45.85, H 4.62, N 14.26; found: C 46.08, H 5.01, N 13.89.

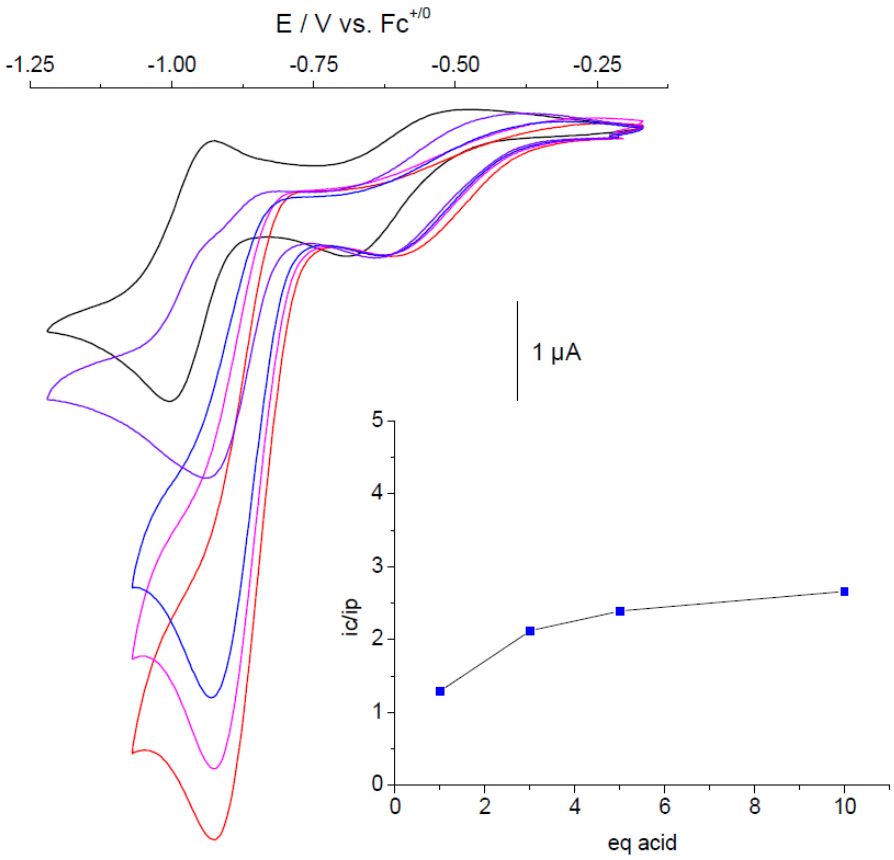

Supplementary Figure S1.Cyclic voltammograms of cobalt complex **3** in the presence of increasing concentrations of anilinium tetrafluoroborate (0, 1, 3, 5, 10 equiv., pK_a = 10.7) in acetonitrile (0.1 M nBu$_4$NBF$_4$ as supporting electrolyte, glassy carbon electrode, scan rate 100 mV·s^{-1}). Electrocatalytic H_2 evolution requires an overpotential of 185 mV. Inset: Plot of *ic/ip* versus acid concentration.

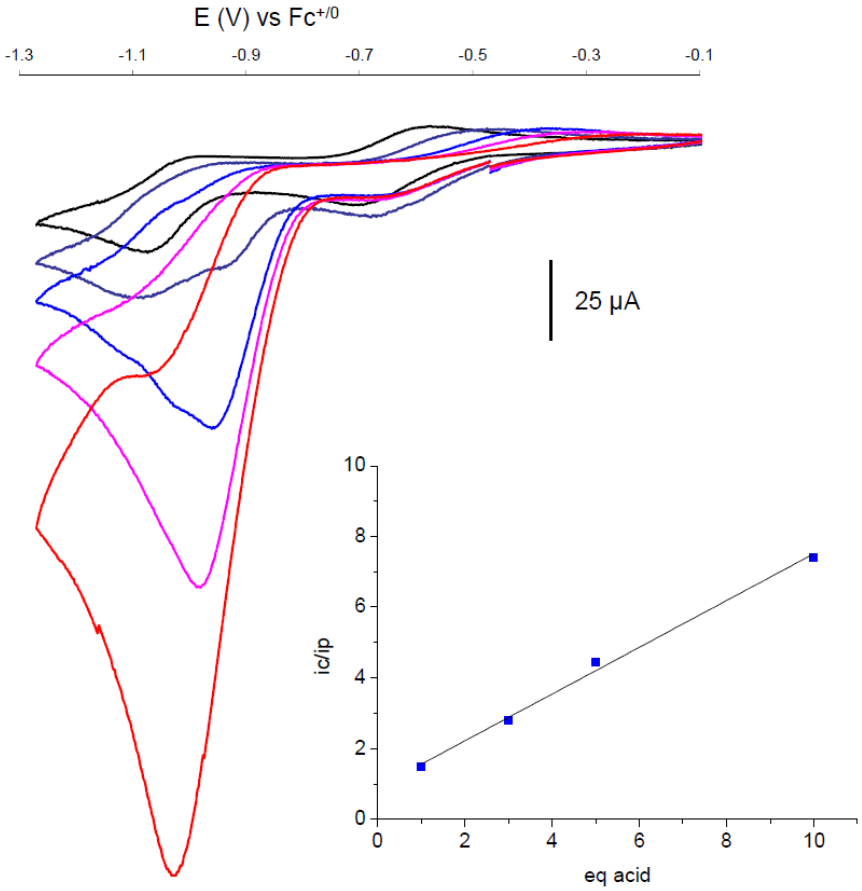

Supplementary Figure S2. Cyclic voltammograms of cobalt complex **2** in the presence of increasing concentrations of anilinium tetrafluoroborate (0, 1, 3, 5, 10 equiv., pK_a = 10.7) in acetonitrile (0.1 M nBu$_4$NBF$_4$ as supporting electrolyte, glassy carbon electrode, scan rate 100 mV·s^{-1}). Electrocatalytic H_2 evolution requires an overpotential of 285 mV. Inset: Plot of *ic/ip* versus acid concentration.

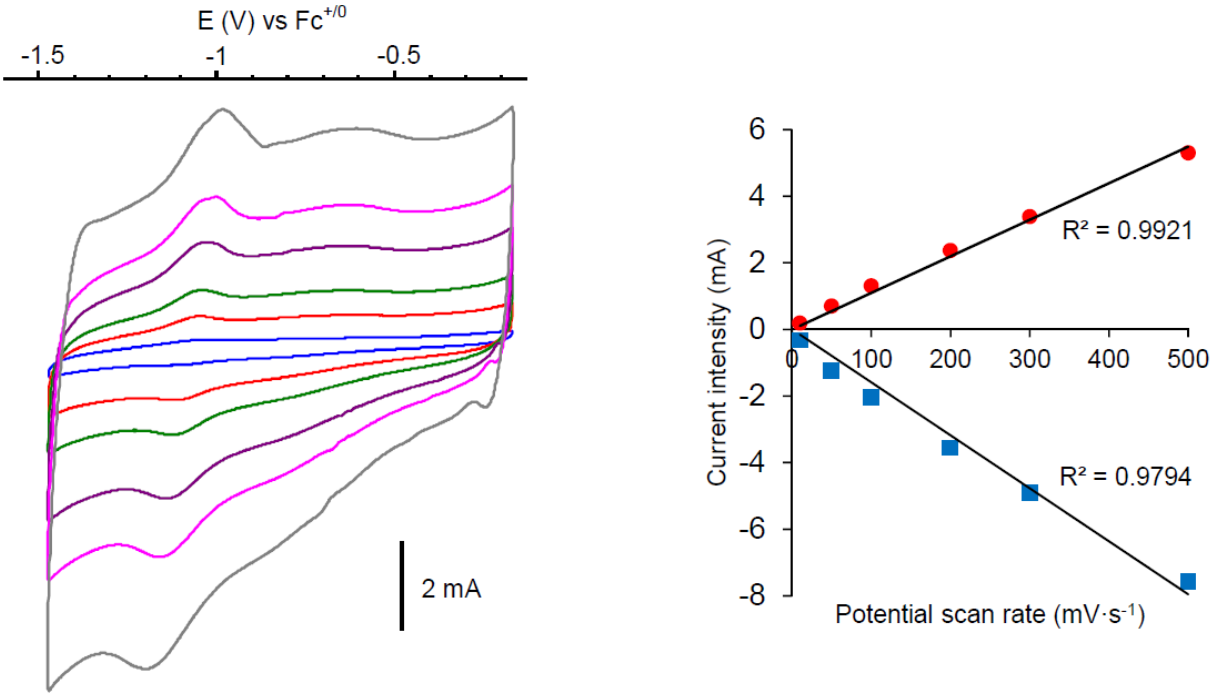

Supplementary Figure S3. *Left:* Cyclic voltammograms recorded at different scan rates (10, 50, 100, 200, 300 and 500 $mV \cdot s^{-1}$) on a GDL/MWCNT/Co electrode (surface catalyst concentration: $4.5 \pm 0.5 \cdot 10^{-9}$ $mol \cdot cm^{-2}$) in acetonitrile (0.1 M Et_4NCl as supporting electrolyte). *Right:* linear evolution with the scan rate of the cathodic and anodic peak current related to the Co^{II}/Co^{I} couple.

Supplementary Table S1. Ratio analysis of the peaks in XPS spectra

	% C	% O	% Co	% N	% Cl
Pristine MWCNTs	97.3	2.7	-	-	-
amino decorated MWCNTs	91.2	4.9	-	3.9	-
cobalt-functionalized MWCNTs	88.9	5.5	0.2	5.1	0.3
3	63.5	10.7	2.3	16.9	6.6
3 (theoretical) $C_{29}H_{35}Cl_2CoN_8O_7$	61.7	14.9	2.1	17.0	4.3

Scofield sensitivity factor used for the calculation:[6] C_{1S}=1; N_{1S} =1.8; O_{1S} =2.93; Cl_{2p}=2.28; $Co_{2p3/2}$=12.62 for Al Kα X-rays.

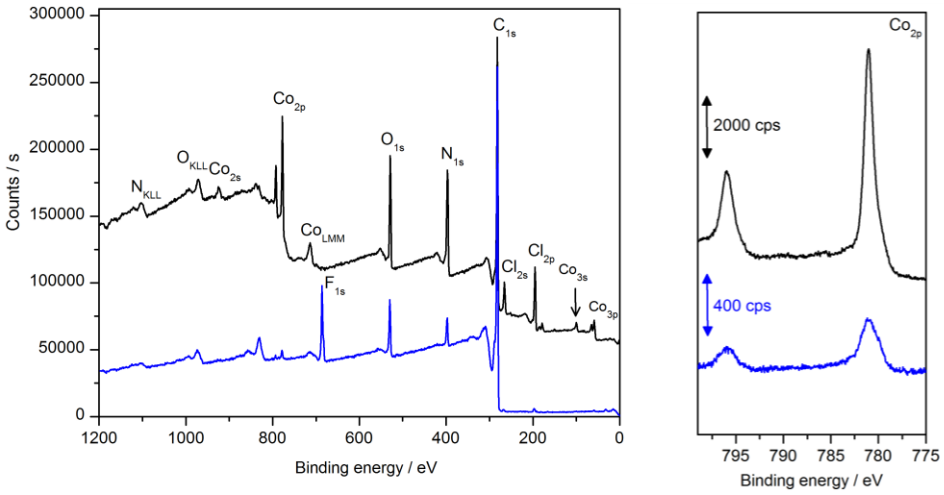

Supplementary Figure S4: XPS survey (left) and Co_{2p} core level spectra (right) of a GDL/MWCNT/Co material (blue) compared to cobalt complex **3** (black).

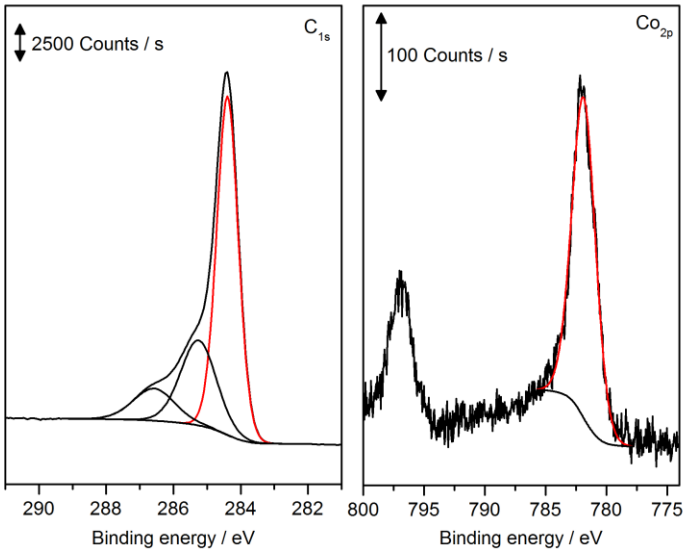

Supplementary Figure S5: Decomposed XPS N 1s and Co 2p spectra of GDL/MWCNT/Co material. Red contributions were used to determine the $Co2p_{3/2}$/C1s ratio.

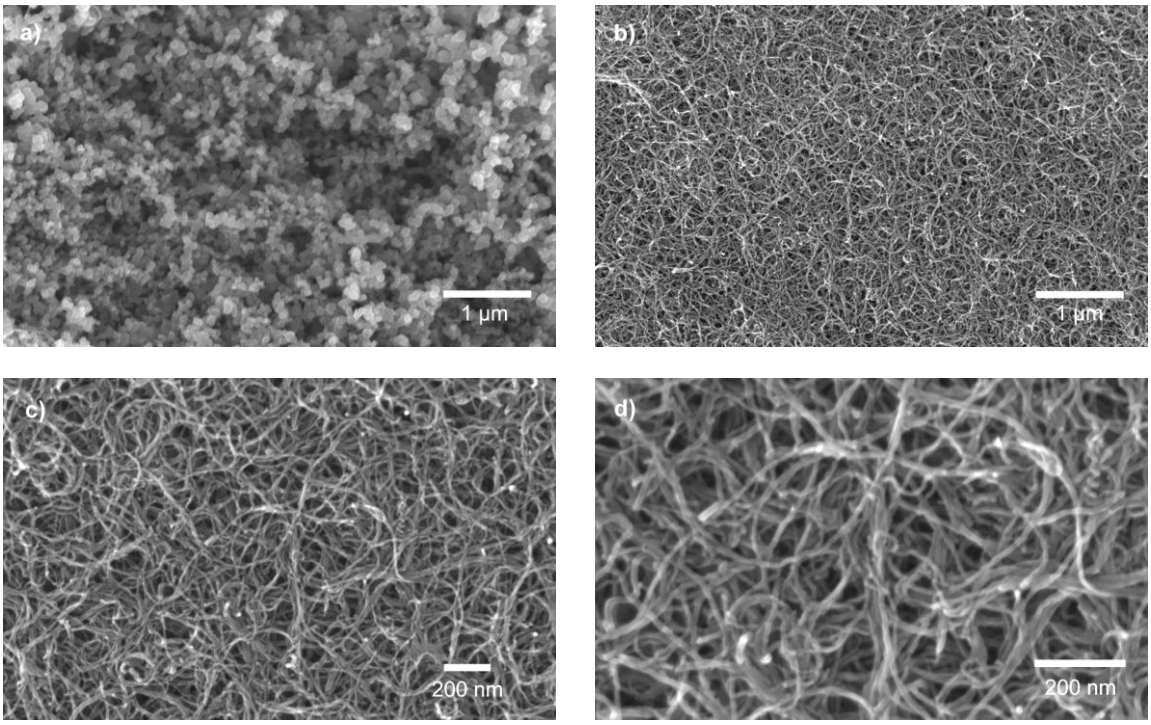

Supplementary Figure S6. Scanning electron micrographs of a GDL electrode (a) and a GDL/MWCNT/Co electrode before (b) and after (c, d) electrolysis at -0.59 V vs. RHE in acetate buffer (0.1 M, pH 4.5), showing the homogeneous, stable deposit of carbon nanotubes (0.2 $mg \cdot cm^{-1}$) and the absence of large conglomerates or metallic nanoparticles.

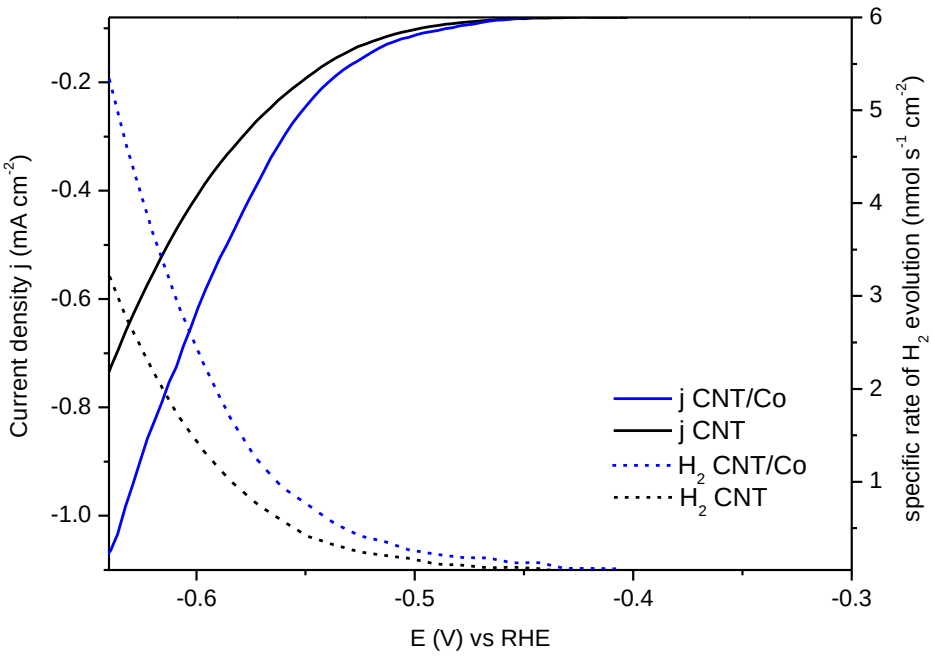

Supplementary Figure S7. Linear sweep voltammetry (plain lines) recorded on a GDL/MWCNT/Co electrode (blue) compared to a blank GDL/MWCNT electrode (black) in phosphate buffer (0.1 M, pH 7.1) at low scan rates (0.1 $mV \cdot s^{-1}$) with simultaneous monitoring of H_2 evolution by gas chromatography (dotted lines).

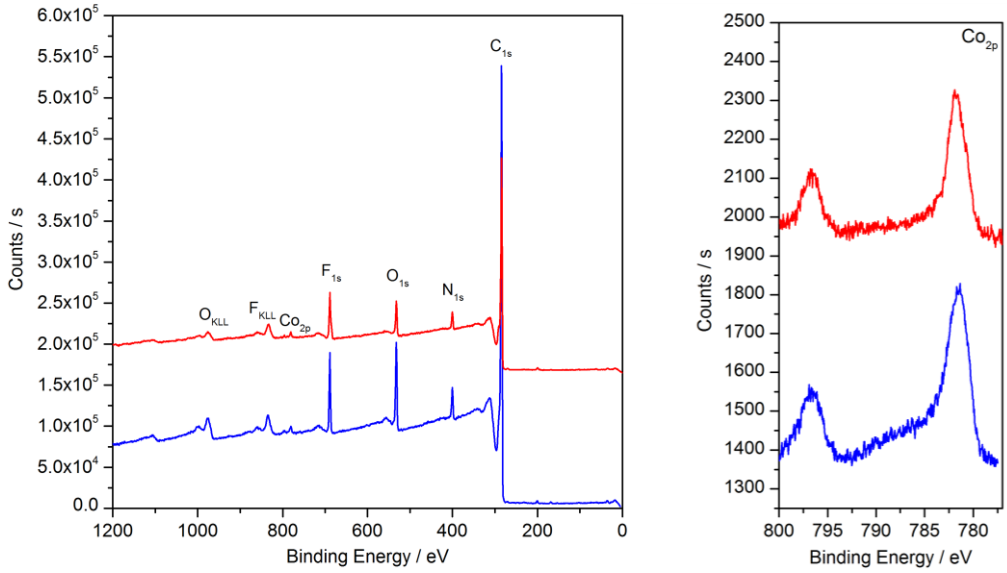

Supplementary Figure S8: XPS survey (left) and Co_{2p} core level spectra (right) of a GDL/MWCNT/Co material before (blue) and after (red) electrolysis at -0.59 V vs. RHE in acetate buffer (0.1 M, pH 4.5).

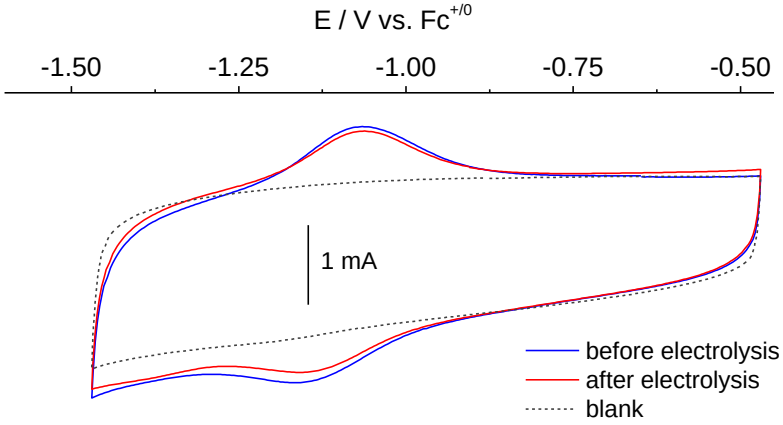

Supplementary Figure S9. Cyclic voltammograms recorded on a GDL/MWCNT/Co electrode in acetonitrile (0.1 M nBu$_4$NBF$_4$ as supporting electrolyte, scan rate 100 mV·s^{-1}) before (black) and after (red) a 4h-electrolysis experiment at -0.59 V vs RHE in acetate buffer (0.1 M, pH 4.5), compared to the blank GDL/MWCNT electrode (dotted).

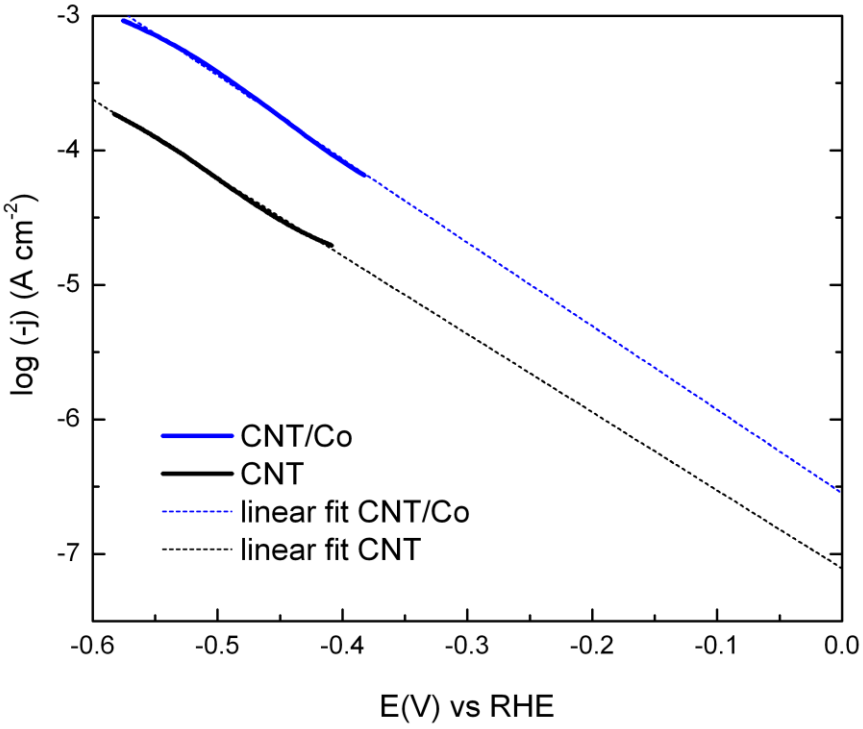

Supplementary Figure S10. Tafel plot derived from the linear sweep voltammetry recorded on a GDL/MWCNT/Co electrode (blue) compared to an unfunctionalized GDL/MWCNT electrode (black) in acetate buffer (0.1 M, pH 4.5) at low scan rates (0.1 $mV \cdot s^{-1}$).

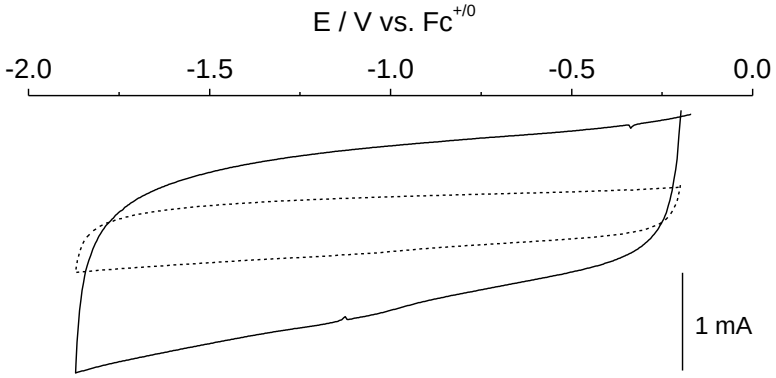

Supplementary Figure S11. Cyclic voltammograms recorded on a blank GDL/MWCNT electrode (solid line) and on a blank GDL electrode (dotted line) in acetonitrile (0.1 M nBu$_4$NBF$_4$ as supporting electrolyte, scan rate 100 mV·s^{-1})

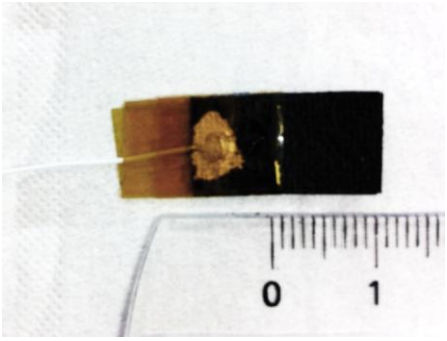

Supplementary Figure S12. Picture of a representative GDL/MWCNT/Co modified electrode.

References

(1) Griveau, S.; Mercier, D.; Vautrin-Ul, C.; Chaussé, A. *Electrochemistry Communications* **2007**, *9*, 2768-2773.
(2) CrysAlisPro CCD, CrysAlisPro RED and ABSPACK; Agilent Technologies: Yarnton, England, 2011
(3) SHELXTL Version 6.1: Sheldrick, G. M. (1997) Bruker AXS Inc., Madison, Wisconsin, USA.
(4) Ramalingam, K.; Raju, N.; Nanjappan, P.; Nowotnik, D. P. *Tetrahedron* **1995**, *51*, 2875-2894.
(5) Sletten, E. M.; Bertozzi, C. R. *Accounts of Chemical Research* **2011**, *44*, 666-676.
(6) Scofield, J. H. *Journal of Electron Spectroscopy and Related Phenomena* **1976**, *8*, 129-137.